

First Demonstration of Highly Reflective and Highly Polarization Selective Diffraction Gratings (GIRO-Gratings) for Long-Wavelength VCSEL's

S. Goeman, S. Boons, B. Dhoedt, K. Vandeputte, K. Caekebeke, P. Van Daele, and R. Baets

Abstract— We present experimental results on surface relief gratings in GaAs and InP with high reflectivity (>85%) and polarization selectivity to normal incidence from the semiconductor side. The potential for polarization stabilization with a reduced mirror complexity for long-wavelength VCSEL's is discussed.

Index Terms— Grating reflectors, semiconductor lasers, surface-emitting lasers.

I. INTRODUCTION

ALTHOUGH short wavelength VCSEL's (850 and 980 nm) are commercially available, most of these devices still show unstable output polarization and transversal multimode behavior [1]. Several solutions have already been proposed to overcome these problems. Using AIAs oxidation in the top distributed Bragg reflector (DBR) mirror offers beside current confinement an improvement of transverse monomodal operation [2]. Concerning the polarization problem, asymmetric etched post structures or growth on (311) substrates have been proposed [3]–[5]. This causes anisotropy of the gain, leading to pinning of the polarization. Also surface relief gratings have been proposed [6], [7].

In this letter, we propose a surface relief structure not only showing polarization selectivity but also a high reflectivity for TM polarization. This property is of specific interest to long-wavelength vertical-cavity surface-emitting lasers (VCSEL's) in view of the low refractive index contrast in these devices leading to rather complex mirror structures (wafer fusion [8], metamorphic growth [9]) and associated electrical and thermal problems. Using the approach presented, it is possible to stabilise the polarization and to decrease the number of DBR pairs of the top VCSEL mirror, possibly leading to a smaller electrical and thermal resistance. In Section II, we will shortly discuss the grating design. Section III describes the fabrication and shows measurement results of GaAs and InP based Giant Reflectivity to Order (GIRO)-gratings. Section IV presents calculations showing that the fabricated GIRO-gratings on top of a reduced DBR stack will lead to complete polarization control.

II. GRATING DESIGN

In this section, we will only briefly discuss the the working principle and design rules of these “GIRO-gratings.” A more

Manuscript received April 7, 1998; revised June 1, 1998. This work was supported in part by the European ACTS024- VERTICAL Project and in part by the Belgian DWTC-Project IUAP- 13. The work of S. Goeman and B. Dhoedt was supported by the Flemish IWT.

The authors are with the Department of Information Technology (INTEC), University of Ghent—IMEC, B-9000 Ghent, Belgium.

Publisher Item Identifier S 1041-1135(98)06299-5.

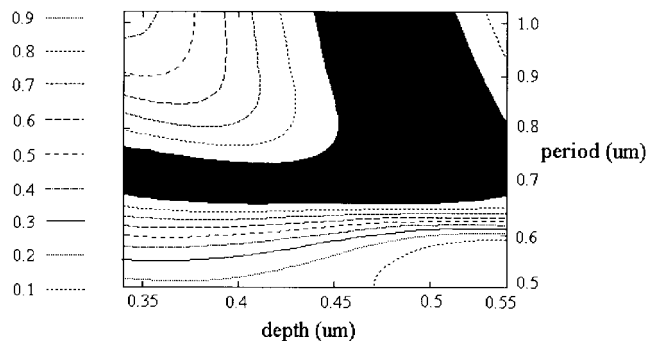


Fig. 1. TM reflectivity GaAs GIRO grating, filling factor 50%. Black region: TM reflectivity >90%, wavelength = 1.55 μm .

detailed study will be explained elsewhere [10]. A GIRO-grating is a linear surface grating between semiconductor and air. A plane wave is incident normal to the grating plane, from the semiconductor side. By choosing the grating period, only the zeroth-order reflection exist in air and there are only two excited propagating optical modes in the grating region. The zeroth-order mode is highly concentrated in the grating ridges and the second-order mode is highly concentrated in the air gaps between the ridges. By choosing the proper grating depth, the average field at the grating air interface composed of these two modes is almost zero and, therefore, no optical power is coupled to the zeroth order in transmission. At the same time, the two optical modes interfere constructively at the grating semiconductor interface thereby coupling almost all power to the zeroth order in reflection and cancelling the higher diffraction orders (in practice, the $-1,1$ and $-2,2$ diffraction order). Ultimately, this leads to the following approximate design rules for such a grating:

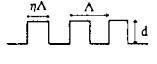
$$n_{e,0} = \sqrt{n_1^2 - (\lambda/\Lambda)^2}, \quad n_{e,2} = n_2$$

$$\frac{\Lambda}{\lambda} = \frac{2}{\sqrt{n_1^2 - n_2^2}}, \quad \frac{d}{\lambda} = \frac{3/2}{\sqrt{3n_1^2 + n_2^2 - n_2}}$$

with $n_{e,0}$ and $n_{e,2}$ the effective indices of the zeroth- and the second-grating mode, λ the vacuum wavelength, Λ the grating period, d the grating depth, n_1 the semiconductor refractive index, n_2 the refractive index of air. We have found that these design rules only work for the TM polarization and not for the TE polarization. The reason for this is the different form of the optical modes for the two polarizations.

In view of the approximations used to arrive at the design rules, we have designed GaAs and InP GIRO gratings for the wavelength of 1.55 μm , using a diffraction model based on rigorous coupled wave analysis [11], using the design rules

TABLE I
GIRO-GRATING PARAMETERS, WAVELENGTH = 1.55 μm

Material	GaAs	InP
	$\Lambda = 900 \text{ nm}$ $d = 500 \text{ nm}$ $\eta = 50\%$	$\Lambda = 880 \text{ nm}$ $d = 525 \text{ nm}$ $\eta = 50\%$

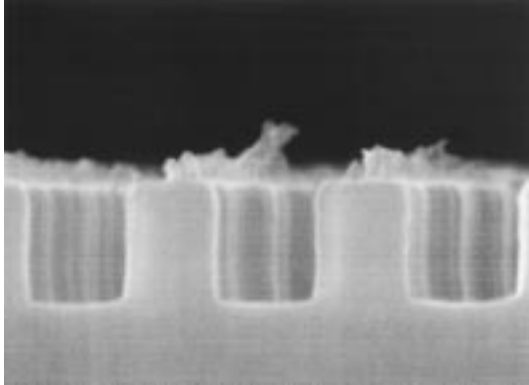


Fig. 2. SEM picture of an InP GIRO grating.

as a starting point. Fig. 1 shows theoretical results for the TM reflectivity of a GaAs grating over a large period and depth range for a grating filling factor of 50%. These results show a large region of high TM reflectivity ($>90\%$). In this region, the TE reflectivity is between 0% and 40%. In view of this large area it is feasible to fabricate highly TM reflective and highly polarization selective gratings. Further calculations have shown it is also possible to achieve GIRO behavior for other filling factors, although, the optimum performance is for filling factors close to 50%. In order to account for possible errors in grating period, depth and filling factor, the parameters of the gratings we choose to fabricate are different from the optimum parameters. The grating parameters are summarized in Table I.

III. FABRICATION AND EXPERIMENTAL RESULTS

As proof of principle, we have first fabricated these gratings for operation with a tuneable CO_2 -laser (9–11 μm) [12]. In this section, we will show experimental results of GaAs and InP based GIRO-gratings for the wavelength region of 1.55 μm . The gratings were fabricated in undoped GaAs and InP using holographic exposure and Ti evaporation, to produce the etch mask, and subsequent reactive ion etching (SiCl_4 for GaAs and CH_4/H_2 for InP). Fig. 2 shows a SEM picture of an InP GIRO-grating. The picture shows a well-defined grating with vertical walls and a filling factor close to 50%. Since we have to evaluate the grating reflectivity from the substrate side, the samples were polished under a wedge angle (3°) to avoid multiple beam interference. This allows us to measure the reflectivity of the polished interface and the grating interface, as seen from the substrate side, separately. The measurements were performed using a tuneable laser (1480–1560 nm). The light is coupled via optical fiber terminated with a gradient index (GRIN) lens to obtain a collimated bundle. After passing a polarizer and a beam splitter, the light is incident on the sample. The reflected light is measured with a detector. The sample is mounted in a rotational setup. First, the reflected power of the polished interface is measured under normal

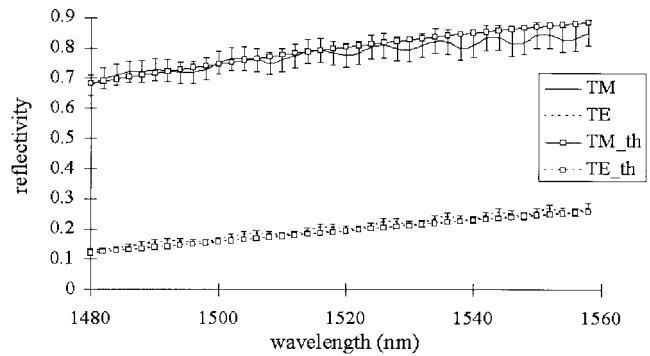


Fig. 3. TM and TE reflectivity of InP GIRO grating and comparison with theory for the wavelengths of 1480–1560 nm.

TABLE II
SEM PARAMETERS AND FITTED PARAMETERS
FOR THE GaAs AND InP GIRO-GRATING

	SEM parameters	fitted parameters
GaAs GIRO-grating	period = 900 nm depth = 450–480 nm filling factor: 40–45 %	period = 900 nm depth = 465 nm filling factor: 45%
InP GIRO-grating	period = 880 nm depth = 580–600 nm filling factor: 50 %	period = 880 nm depth = 580 nm filling factor: 50%

incidence. The sample is rotated so that that the incident beam is normal to the grating interface and the reflected power of the grating interface is measured. This results in the following relation:

$$R_{\text{gr}} = \frac{R_0^\circ P_{\text{gr}}}{T_\theta^2 P_{\text{pi}}}$$

With P_{pi} , the reflected power measured from the polished interface, P_{gr} the reflected power from the grating interface, R_0 the Fresnel reflection coefficient under 0° and T_θ the Fresnel transmission coefficient under θ degrees incidence. We assume these coefficients to be $R_{0,\text{TE}} = 0.295$, $T_{\theta,\text{TE}} = 0.698$, $R_{0,\text{TM}} = 0.295$, $T_{\theta,\text{TM}} = 0.713$ for GaAs ($R_{0,\text{TE}} = 0.271$, $T_{\theta,\text{TE}} = 0.722$, $R_{0,\text{TM}} = 0.271$, $T_{\theta,\text{TM}} = 0.737$ for InP), assuming a refractive index of undoped GaAs of 3.3737 (3.17 for InP) [13]. Using this equation, it is possible to determine the grating reflectivity for both polarizations and compare it with theoretical calculations.

Fig. 3 shows the measurement results (error bar of $\pm 5\%$) and a comparison with theoretically calculated values for an InP GIRO-grating. The calculations agree well with the measurements (almost within the measurement error) and the grating parameters used in the calculations agree well with the SEM parameters (Table II). This grating shows a maximum TM reflectivity of 85% for $\lambda = 1550 \text{ nm}$ and polarization selectivity of more than 60% over the entire wavelength region. Fig. 4 gives the measurement results and a comparison with theory for the GaAs GIRO grating. The polarization selectivity of this grating is more than 50% over the whole wavelength region and the maximum TM reflectivity is 85% for $\lambda = 1490 \text{ nm}$. As for the InP grating, the calculations agree well with the measurement (within the measurement error) and again, the grating parameters used in the calculations agree well with the SEM parameters (Table II).

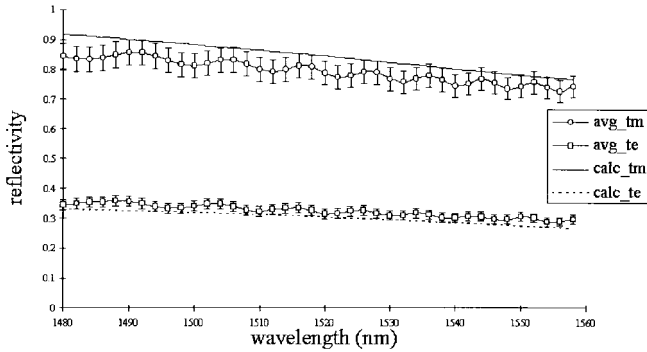


Fig. 4. TM and TE reflectivity of GaAs GIRO grating.

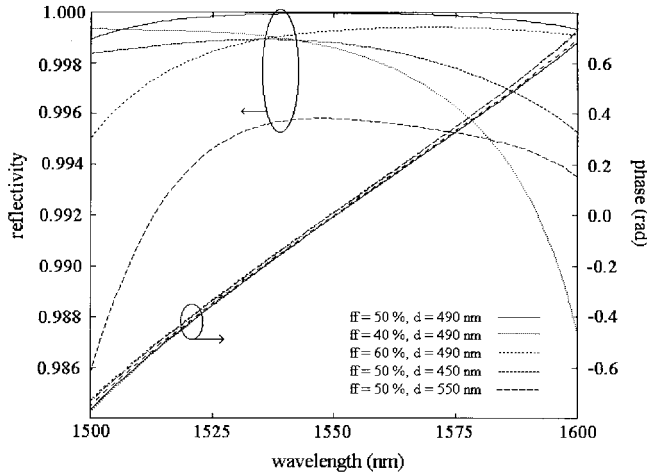


Fig. 5. Reflectivity and phase for 5 different situations of filling factor and grating depth ($ff = 50\%$ $d = 490$ nm, $ff = 40\%$ $d = 490$ nm, $ff = 60\%$ $d = 490$ nm, $ff = 50\%$ $d = 450$ nm, $ff = 50\%$ $d = 550$ nm).

IV. COMBINATION OF GIRO + DBR FOR TOP VCSEL MIRROR

The controlled fabrication of highly reflecting DBR mirrors is a key factor in VCSEL operation. Improvements in epitaxial layer growth have made it possible to fabricate these DBR mirrors. Technologically, the fabrication of grating structures is not so well controlled. The main problems are the grating filling factor and the grating depth. Although theoretically the TM reflectivity of a GIRO-grating is high enough (and high polarization selectivity) in practise, we will still need some additional DBR pairs to ensure that the reflectivity is not too sensitive to the grating filling factor and the grating depth. Another problem we have not addressed, so far, is the phase behavior of these GIRO-gratings. In this section, we examine the sensitivity of the reflection and the phase of a top VCSEL mirror consisting of a GIRO grating on top of a reduced DBR stack. Since the underlying DBR stack will decrease the polarization selectivity we want to find out what the remaining polarization selectivity will be. Fig. 5 shows the reflectivity and phase as a function of wavelength for a 13.5 pair AlAs–GaAs DBR stack, a GaAs phase matching layer of 135 nm and the GaAs GIRO grating on top (period = 900 nm, depth = 490 nm). Five different situations are considered (constant depth 490 nm and filling factors 50%, 40%, and 60%; constant filling factor 50% and grating depth 450, 490, 500 nm). In these calculations, the thickness of the top GaAs layer is constant (625 nm) as it would be in real situations.

Fig. 5 shows that the reflectivity remains higher than 99.5% for the different filling factors and grating depths. For all five situations, the TE reflectivity is 0.5%–2% smaller over the complete wavelength region. The phase of the TM reflection as a function of wavelength is comparable for all situations and is approximately the same as for a pure DBR stack. This means that the grating parameters do not influence the phase much. So, accurate growth of the complete layer structure will be more for determining the cavity resonance wavelength.

V. CONCLUSION

In this letter, we have described the design, fabrication and experimental results of highly polarization selective and highly TM reflective gratings in GaAs and InP. The experiments show reflectivities of 85% and these results are in good agreement with theoretical calculations. Furthermore we have indicated the potential of these gratings for long wavelength VCSEL's; in combination with a DBR stack, these gratings would lead to a reduced number of DBR pairs and a remaining polarization selectivity in the order of 0.5%–2%.

REFERENCES

- [1] C. J. Chang-Hasnain, J. P. Harbison, G. Hasnain, A. C. Von Lehmen, L. T. Florez, and N. G. Stoffel, "Dynamic, polarization, and transverse mode characteristics of vertical cavity surface emitting lasers," *IEEE J. Quantum Electron.*, vol. 27, pp. 1402–1409, June 1991
- [2] K. L. Lear, K. D. Choquette, R. P. Schneider, S. P. Kilcoyne, and K. M. Geib, "Selectively oxidised vertical cavity surface emitting lasers with 50% power conversion efficiency," *Electron. Lett.*, vol. 31, no. 3, pp. 208–209, Feb. 1995.
- [3] T. Yoshikawa, H. Kosaka, K. Kurihara, M. Kajita, Y. Sugimoto, and K. Kasahara, "Complete polarization control of 8x8 vertical-cavity surface-emitting laser matrix arrays," *Appl. Phys. Lett.*, vol. 66, no. 8, pp. 908–910, Feb. 1995.
- [4] T. Mukaiharu, F. Koyama, and K. Iga, "Engineered polarization control of GaAs/AlGaAs surface-emitting lasers by anisotropic stress from elliptical etched substrate hole," *IEEE Photon. Technol. Lett.*, vol. 5, pp. 133–135, Feb. 1993.
- [5] M. Takahashi, N. Egami, T. Mukaiharu, F. Koyama, and K. Iga, "Lasing characteristics of GaAs(311)A substrate based InGaAs-GaAs vertical-cavity surface-emitting lasers," *IEEE J. Select. Topics Quantum Electron.*, vol. 3, pp. 372–378, Apr. 1997.
- [6] T. Mukaiharu, N. Ohnoki, Y. Hayashi, F. Koyama, and K. Iga, "Polarisation control of vertical-cavity surface-emitting lasers by birefringent metal/semiconductor polarizer terminating a distributed Bragg reflector," in *Proc. IEEE ISLC'94*, Maui, HI, p. 183, paper W1.6.
- [7] J. H. Ser, Y. G. Ju, J. H. Shin, and Y. H. Lee, "Polarization stabilisation of vertical-cavity top-surface-emitting lasers by inscription of fine metal-interlaced gratings," *Appl. Phys. Lett.*, vol. 66, no. 21, pp. 2769–2771, May 1995.
- [8] D. I. Babic, K. Streubel, R. P. Mirin, N. M. Margalit, M. G. Peters, J. E. Browsers, E. L. Hu, "Fabrication and Characteristics of double-fused vertical-cavity lasers," *Opt. Quantum Electron.*, vol. 28, pp. 475–485, 1996.
- [9] H. Gebretsadik, K. Kamath, K. Linder, and P. Bhattacharya, "Defect-Free GaAs/AlAs Distributed Bragg Reflector Mirrors on patterned InP-Based Heterostructures: Application to 1.55 μm VCSELs," in *Proc. IEEE LEOS'97*, San Francisco, CA, p. 305, paper TuU3.
- [10] B. Dhoedt, S. Goeman, B. Demeulenaere, B. Baekelandt, D. De Zutter, and R. Baets, "GIRO gratings: a novel concept for mirrors with high reflectivity and polarisation selectivity," *Diffraction Optics Micro-Optics'96*, postdeadline paper J Tu B30.
- [11] M. G. Moharam, D. A. Pommert, and E. B. Grann, *J. Opt. Soc. Amer.*, vol. 12, no. 5, pp. 1077–1086, May 1995.
- [12] S. Goeman, B. Dhoedt, K. Caekebeke, S. VERstuyft, R. Baets, P. Van Daele, N. Nieuborg, K. Panajotov, H. Thienpont, "Experimental demonstration of high TM reflectivity in GaAs based GIRO-gratings in the wavelength region of 9–11 μm ," *IEEE LEOS'97*, San Francisco, CA, p. 13, paper MA5.
- [13] E. Palik, *Handbook of Optical Constants of Solids*. New York: Academic (Handbook Ser.), 1985.